Predictions of Mechanical Properties of Quenched and Tempered Steel

Božo Smoljan[*] - Dario Iljkić - Furio Traven
University of Rijeka, Faculty of Engineering, Department of Materials Science and Engineering, Croatia

Mechanical properties of quenched steel directly depend on the degree of quenched steel hardening. Fracture toughness and fatigue limit depend on microstructural constituents, and distribution of the usual intermetallic particles and non-metallic inclusions. Fatigue resistance of quenched and tempered steel is achieved by eliminating coarse alloy carbides present in steel. Properties of matrix may also have an important influence on fracture and fatigue proper behaviour. Most high-strength materials are fracture and fatigue limited. Fatigue strength is directly proportional to the difficulty of dislocation cross slip. Grain size has its greatest effect on fatigue life in the low-stress, high-cycle regime.

In this paper, fatigue crack initiation threshold of quenched and tempered steel is predicted. The method of computer simulation of mechanical properties was applied for a workpiece of complex form made of quenched and tempered steel. Distribution of as-quenched hardness within workpiece of complex form was predicted by computer simulation of steel quenching using the finite volume method. Microstructure composition and hardness of tempered steel were predicted based on as-quenched hardness. Fatigue crack initiation threshold of quenched and tempered steel were predicted based on microstructure composition and hardness.

It was found that the proposed method can be successfully applied in calculating fatigue crack initiation threshold of quenched and tempered steel.

0 INTRODUCTION

The numerical simulation of hardness distribution in quenched steel specimen is one of the highest priorities in simulating the phenomena of steel quenching and in predicting the mechanical properties of quenched steel specimen. Strength, toughness and fatigue properties can be estimated based on steel hardness [1]. Prediction of hardness, strength, and fatigue crack initiation threshold distribution in quenched steel specimen will be made by computer simulation.

Strength, toughness and fatigue properties of quenched and tempered steel directly depend on steel microstructure. For that reason, two main problems have to be solved in simulating steel quenching: prediction of temperature field change, and prediction of microstructure composition and mechanical properties. The mathematical model of steel quenching can be based on calculated characteristic time of cooling from 800 to 500°C, $t_{8/5}$ [2] and [3]. The hardness at specimen points can be estimated by the conversion of cooling time results to hardness by using both, the relation between cooling time and distance from the quenched end of *Jominy* specimen and the *Jominy* hardenability curve. The time of cooling at specimen point can be predicted by the numerical simulation of cooling using the finite volume method [4] and [5].

1 PREDICTION OF FATIGUE PROPERTIES

The structural transformation and mechanical properties can be estimated based on time relevant for structure transformation. The as-quenched hardness at specimen points can be estimated by the method explained in reference [6] based on cooling time $t_{8/5}$.

The referent hardness at specimen points in the quenched and tempered state can be estimated from the referent as-quenched hardness, $HRC_{quenched}$, by [7] and [8]:

$$HRC_{tempered} = \frac{HRC_{quenched}}{K} .$$ (1)

Factor K can be expressed by:

$$K = C_1 \cdot t^{n_1} \exp\left[A\left(\frac{a}{T_{temp}}\right)^{n_2} - B \right],$$ (2)

[*]Corr. Author's Address: Faculty of Engineering, Vukovarska 58, 51000 Rijeka, Croatia, smoljan@riteh.hr

where T_{temp} [K] is the tempering temperature, t [h] is the time, while A, B, C_1, a, n_1 and n_2 are the material constants that are established by regression analysis of hardness of quenched and tempered steel. Eqs. (1) and (2) are valid for carbon and low alloy steel.

The results of austenite decomposition depend on the chemical composition of steel, severity of cooling, austenitizing temperature and steel history. In accordance with reference [9] three kinds of basic structures are observed in CCT diagrams: martensite, bainite, and ferrite-pearlite. Microstructure composition of steel is in relation with actual steel hardness. Steel hardness is generally equal [9]:

$$HV = \left\{ \left(\%ferrite + \%pearlite \right) HV_{(F+P)} + \right.$$
$$\left. + \left(\%bainite \right) HV_{(B)} + \left(\%martensite \right) HV_{(M)} \right\} /100. \quad (3)$$

Amount of phases's volume portions is equal unity:

$$\left\{ \left(\%ferrite + \%pearlite \right) + \right.$$
$$\left. + \%bainite + \%martensite \right\} /100 = 1. \quad (4)$$

If the total hardness and the hardness of microstructure constituents are known, and if the phase fraction of one of microstructure constituents is known, it is not difficult to predict fractions of other phases by the Eqs. (3) and (4). The austenite decomposition results can be estimated based on time relevant for structure transformation.

The characteristic cooling time, relevant for structure transformation for most structural steels, is the time $t_{8/5}$. If other heat treatment parameters are constant, the austenite decomposition results in some location of a cooled specimen will depend only on the time $t_{8/5}$. Phase hardness for *Jominy* specimen depends on chemical composition and cooling rate parameter that corresponds to actual distance d of *Jominy* specimen quenched end. It has been adopted that cooling rate parameter is equal to $\log(t_{8/5})$ and hardnesses of basic phases, i.e., martensite, bainite, and ferrite-pearlite are equal to [10]:

$$HV_d^M = HV_{max}^M - K_M \log \frac{t_{8/5d}^M}{t_{8/5\,max}^M}, \quad (5)$$

$$HV_d^B = HV_{max}^B - K_B \log \frac{t_{8/5d}^B}{t_{8/5\,max}^B}, \quad (6)$$

$$HV_d^{P+F} = HV_N^{P+F} + K_{P+F} \log \frac{t_{8/5N}^{P+F}}{t_{8/5d}^{P+F}}, \quad (7)$$

where N is normalizing, and HV_{max}^B is hardness of lower bainite. Characteristic values of HV_{max}^M, HV_{max}^B, HV_N^{P+F}, K_M, K_B, K_{P+F}, $t_{8/5max}^M$, $t_{8/5max}^B$, $t_{8/5N}^{P+F}$, $t_{8/5d}^M$, $t_{8/5d}^B$ and $t_{8/5d}^{P+F}$ in Eqs. (5), (6) and (7) have to be evaluated for investigated steel based on *Jominy* test results and the relation between time of cooling from 800 to 500°C $t_{8/5}$, and the Jominy distance [11]. Hardness of quenched structures with characteristic percentage of martensite can be predicted by using the diagram of hardness at different percentages of martensite vs. carbon content after Hodge and Orehoski [12] and [13] and *Jominy* curve. The regression relations between the time $t_{8/5}$ and characteristic pearlite fractions are established [10].

Mechanical properties of quenched steel or quenched and tempered steel directly depend on the degree of quenched steel hardening [1]. The relation between hardness, HV, and yield strength, $R_{p0.2}$ [Nmm^{-2}] is equal to [6]:

$$R_e = R_{p0,2} = \left(0.24 + 0.03C \right) HV + 170C - 200, \quad (8)$$

where C is the degree of hardening is defined as the ratio of the measured hardness after quenching to the maximum hardness that can be achieved with the actual steel [14].

Fatigue crack initiation threshold, ΔK_{th} could be estimated based on yield strength and microstructural constitution. The effect of tempering and microstructure composition is relatively small for region 2 growth rates, but the effect may be large near the threshold in region 1 growth rates. Continuous ferrite phase reduces fatigue crack growth resistance near the threshold. Therefore, a substantial reduction in fatigue crack growth resistance near the threshold is possible with segregation of ferrite phase in form of continuous network.

For the low- to medium-strength steels, it is useful to compare the grain size with the reversed plastic zone size, $R_{p\pm}$ [15] to [18]. Controlling microstructural unit for low- to medium-strength steels is reversed plastic zone size, $R_{p\pm}$, which is useful to compare with the grain size. Using twice the plane-strain plastic radius and twice the yield stress due to the stress reversal gives [15]:

$$R_{p\pm} = \frac{2\Delta K^2}{6\pi(2R_e)^2} \ . \tag{9}$$

Cyclic slip will not proceed if the grain size, d, is greater than the reversed plastic zone size. Substituting that $d = R_{p\pm}$, the fatigue crack initiation threshold, ΔK_{th}, below which fatigue cracks would not initiate at specimen points in the quenched and tempered state, can be estimated by [15]:

$$\Delta K_{th} = R_e(12\pi d)^{1/2} = 6.14 R_e d^{1/2} \ . \tag{10}$$

For ferritic-pearlitic microstructure grain size refers to ferritic grain size, but for tempered martensite grain size refers to prior-austenite grain size [15] and [19]. The effects of ferrite-pearlite volume portion in as-quenched microstructure on fatigue crack initiation threshold, ΔK_{th} could be expressed by:

$$\Delta K_{th} = nA_1 R_e d^{1/2} \ , \tag{11}$$

where n is the parameter depending of ferrite-pearlite volume portion in as-quenched microstructure, while A_1 is the material constant derived from Eq. (10). For example, if ferrite-pearlite volume portion equals 10% parameter n equals 0.6.

If threshold values were normalized by grain size and plotted against yield strength, the slope of this curve could then be compared with Eq. (10). The data plotted in this manner predict parameter A_1 equaling 5.0 instead of 6.14. Further experimental work is needed for the final verification of represented model.

2 PRACTICAL EXAMPLE FOR PREDICTING MECHANICAL PROPERTIES FOR QUENCHED AND TEMPERED STEEL

The established method is applied in failure analysis of quenched and tempered steel shaft made of steel 42CrMo4 (DIN). The chemical composition of steel is 0.38 %C, 0.23 %Si, 0.64 %Mn, 0.019 %P, 0.013 %S, 0.99 %Cr and 0.16 %Mo. *Jominy* test results of steel 42CrMo4 are shown in Table 1.

Geometry and failure of the quenched workpiece are shown in Figs. 1 and 2, respectively.

The shaft was treated by two heat treatments: in the first, after heating to 850°C for 1 hour, the shaft was quenched in oil with the severity of quenching $H = 0.25$, and in the second treatment, the shaft was quenched in oil with severity of quenching $H = 0.7$. The tempering temperature was 600°C. The shaft treated by the first heat treatment was broken after a short time of application.

Based on the proposed mathematical model, a computer simulation of microstructure composition and fatigue crack initiation threshold was done.

Table 1. *Jominy test results of investigated steel 42CrMo4*

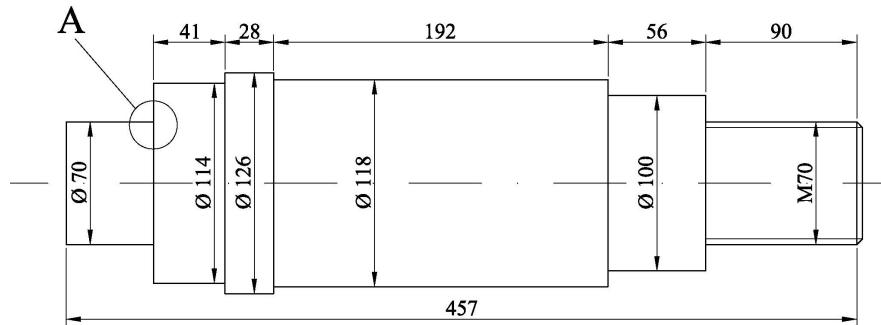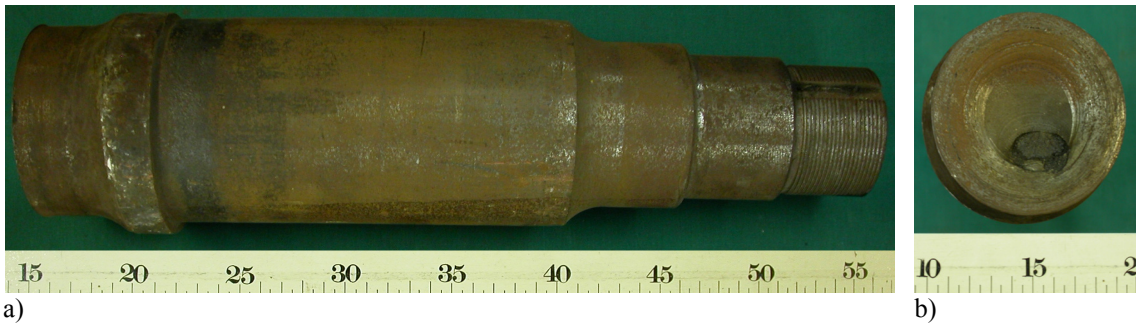| Jominy distance [mm]	1.5	3	5	7	9	11	13	15	20	25	30
Hardness [HV]	610	605	590	576	555	524	487	446	379	344	324
Jominy distance [mm]	35	40	45	50	55	60	65	70	75	80	-
Hardness [HV]	311	303	297	293	292	291	289	288	288	288	-

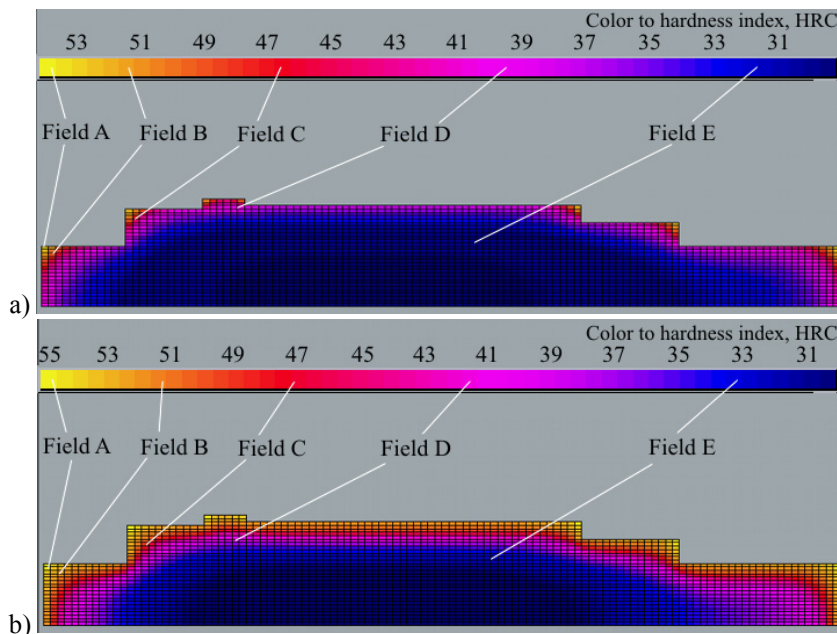

Fig. 1. *Workpiece geometry*

Fig. 2. *Workpiece failure*

Fig. 3. *Distributions of as-quenched hardness (a) for quenching in oil; H = 0.25, (b) for quenching in oil; H = 0.7 in Rockwell units (HRC), from which hardness in Vickers units (HV), yield strength R_e (Nmm^{-2}) and microstructure phase (vol %) have been calculated - see Tables 2 and 3*

Characteristic time $t_{8/5}$ was calculated by the numerical method explained in reference [5]. In the applied mathematical model of quenching values of heat transfer coefficient were calibrated for Grossmann *H*-value equal to 0.25 and 0.7 [5]. Fig. 3 shows distributions of as-quenched hardness in Rockwell units (HRC), from which hardness in Vickers units (HV), yield strength $R_{p0.2}$ [Nmm^{-2}] and microstructure phase volume portion have been calculated. The predicted values of as-quenched microstructure and mechanical properties of the workpiece are given in Table 2 for quenching in oil with the severity of quenching H = 0.25, and in Table 3, for quenching in oil with severity of quenching H = 0.7.

The predicted values of mechanical properties of the workpiece quenched in oil with severity of quenching H = 0.7, subsequently tempered at 600 °C, are given in Table 4. It is observed that near the workpiece surface the as-quenched microstructure of homogeneous martensite is achieved by quenching in oil with severity of quenching H = 0.7 (Fig. 3b). More heterogeneous as-quenched microstructure in surface locations is achieved by quenching in oil with the severity of quenching H = 0.25 (Fig. 3a), which leads to reduced fatigue crack initiation threshold.

By economical aspects of simulation of investigated shaft manufacturing, most suitable

Table 2. *Microstructure and mechanical properties of the as-quenched workpiece for quenching in oil; H = 0.25*

Properties		Field in Fig. 3a				
		A	**B**	**C**	**D**	**E**
Hardness [HV]		610-575	575-510	510-440	440-340	340-290
Yield strength, R_e [MPa]		2013-1898	1898-1683	1683-1452	1452-1122	1122-957
Phase fractions [%]	F+P	0	0	0	0	0-12
	B	1-2	2-19	19-42	42-74	74-83
	M	99-98	98-81	81-58	58-26	26-5

Table 3. *Microstructure and mechanical properties of the as-quenched workpiece for quenching in oil; H = 0.7*

Properties		Field in Fig. 3b				
		A	**B**	**C**	**D**	**E**
Hardness [HV]		610-575	575-510	510-453	453-370	370-298
Yield strength, R_e [MPa]		2013-1898	1898-1683	1683-1495	1495-1221	1221-983
Phase fractions [%]	F+P	0	0	0	0	0-10
	B	1-2	2-19	19-37	37-64	64-81
	M	99-98	98-81	81-63	63-36	36-9

Table 4. *Mechanical properties of the quenched (H = 0.7) and tempered workpiece*

Properties	Field in Fig. 3b				
	A	**B**	**C**	**D**	**E**
Hardness [HV]	291-290	290-280	280-272	272-256	256-234
Yield strength, R_e [MPa]	960-957	957-924	924-898	898-845	845-772
Fatigue threshold, ΔK_{th} [MPam$^{1/2}$]	22.6-22.5	22.5-21.8	21.8-21.2	21.2-20.1	20.1-10.5

shaft manufacture process is to manufacture the shaft from the quenched and tempered bar of 130 mm diameter. But in this case, in critical location A (Fig. 1), heterogeneous microstructure of ferrite, perlite, bainite and martensite will be achieved, with very low fatigue limit.

3 SUMMARY

A mathematical model for prediction of fatigue crack initiation threshold of quenched and tempered steel was developed. The mathematical model has been applied in failure analysis of a quenched and tempered steel shaft. The hardness distribution in the quenched workpiece is estimated based on cooling time from 800 to 500°C, $t_{8/5}$, and on results of the *Jominy* test. The computer program used for predicting the time of cooling, $t_{8/5}$ is based on finite volume method. The prediction of distribution of microstructure composition and yield strength is based on estimated steel hardness. Fatigue crack initiation threshold is predicted based on yield strength and microstructural constitution. Further experimental work is needed to verify the proposed model.

Mechanical properties of quenched and tempered steel workpieces can be successfully calculated by the proposed method, and that the proposed method can be successfully applied in failure analysis of quenched and tempered steel workpieces. For efficient estimation of fatigue crack initiation threshold additional data about microstructure are needed.

Using a numerical simulation of microstructure and mechanical properties, it was established that better results of fatigue crack initiation threshold can be achieved by quenching in oil with higher severity of quenching.

4 REFERENCES

[1] Smoljan, B. (2006) Prediction of mechanical properties and microstructure distribution of quenched and tempered steel shaft. *Journal of Materials Processing Technology*, vol. 175, no. 1, p. 393-397.

[2] Smoljan, B. (1999) The calibration of the heat conductivity coefficient in mathematical model of steel quenching. *Proceedings of MicroCAD `99*, Miskolc.

[3] Smoljan, B. (1995) The calibration of the mathematical model of steel quenching. *Proceedings of 5th World Seminar on Heat Treatment and Surface Engineering*, Isfahan.

[4] Patankar, S. (1980) *Numerical heat transfer and fluid flow*, New York: McGraw Hill Book Company.

[5] Smoljan, B. (1998) Numerical simulation of as-quenched hardness in a steel specimen of complex form. *Communications in Numerical Methods in Engineering*, vol. 14, no. 1, p. 277-285.

[6] Smoljan, B. (2002) Numerical simulation of steel quenching. *Journal of Materials Engineering and Performance*, vol. 11, no. 1, p. 75-80.

[7] Smoljan, B. Smokvina Hanza, S., Iljkić, D., Totten, G. E., Felde, I. (2008) Computer simulation of mechanical properties of steel dies. *Proceedings of 2nd International Conference on Heat Treatment and Surface Engineering of Tools and Dies*.

[8] Reti, T., Felde, I., Guerrero, M., Sarmiento, S. (2009) Using generalized time-temperature parameters for predicting the hardness change occurring during tempering. *Proceedings of the International Conference on New Challenges in Heat Treatment and Surface Engineering*.

[9] Filetin, T. (1992) Calculation of mechanical properties according to Blondeu, Maynier; Dollet and Vieillard-Baron, *Theory and technology of quenching*, Liščić, B., Tensi, H., Luty, W. (eds.), Springer-Verlag.

[10] Smoljan, B. (2002) Computer simulation of microstructure transformation during the quenching. *Proceedings of 1st International Surface Engineering Congress and 13th IFHTSE Congress*, Columbus.

[11] Rose, A. et al. (1954) Atlas for heat treatment of steels I, vol. 2, VDI, Verlag Stahleisen, Düsseldorf. (in German)

[12] Spies, H.J. (1992) Mechanical properties of ferrous and nonferrous alloys after quenchig, *Theory and technology of quenching*, Liščić, B., Tensi, H., Luty, W. (eds.), Springer-Verlag, Berlin.

[13] Smoljan, B., Butković, M. (1998) Simulation of mechanical properties of hardened steel. *Proceedings of MicroCAD '98*, Miskolc.

[14] Just, E. (1976) *Heat treatment – Material effects on quenching and tempering*, VDI Berichte, no. 256, p. 125-140.(in German)

[15] Wilson, A. (1996) Fatigue and fracture resistance of ferrous alloys in *ASM Handbook-Volume 19: Fatigue and fracture*, ASM International, Material Park, OH.

[16] Beevers, C.J. (1977) Fatigue crack growth characteristics at low stress intensities of metals and alloys, *Met. Sci.,* p. 362-367.

[17] Yuen, A., Hopkins, S.W., Leverant, G.R., Rau, C.A. (1974) Correlations between fracture surface appearance and fracture mechanics parameters for stage II fatigue crack propagation in Ti-6Al-4V, *Met. Trans.,* vol. 5, p. 1833-1842.

[18] Cooke, R.J., Irving, P.E., Booth, C.S., Beevers, C.J. (1975) The slow fatigue-crack growth and threshold behavior of a medium-carbon alloy steel in air and vacuum, *Eng. Fract. Mech.*, vol. 7, p. 69-77.

[19] Ritchie, R.O. (1979) Near-threshold fatigue-crack propagation in steels, *International Metals Reviews,* vol. 24, no. 5-6, p. 205-230.